Food Innovation and Advances

ARTICLE

Open Access

https://doi.org/10.48130/fia-0026-0017

Food Innovation and Advances **2026**, 5(2): 251–260

A metabolic optimization strategy based on modular genomic integration of the MVA pathway to enhance lycopene production in *Escherichia coli*

Wanpeng Xia[1,2], Wenqian Li[1,3], Qiang Yao[4] and Jingyu Chen[1,2*]

[1] *College of Food Science and Nutritional Engineering, China Agricultural University, Beijing 100083, China*
[2] *China Agricultural University-Sichuan Advanced Agricultural & Industrial Institute, Chengdu 611430, China*
[3] *School of Health and Life Sciences, University of Health and Rehabilitation Sciences, Qingdao 266113, China*
[4] *State Key Laboratory of Nutrient Use and Management/Institute of Agricultural Resources and Environment, Shandong Academy of Agricultural Sciences, Jinan 250100, China*

* Correspondence: chenjy@cau.edu.cn (Chen J)

Abstract

Lycopene, a bioactive tetraterpenoid antioxidant valued in food, pharmaceutical, and cosmetic sectors, remains constrained by low plant extractability and expensive chemical synthesis; microbial engineering now presents a cost-effective alternative. In this study, key genes from the methylerythritol phosphate (MEP) pathway—*dxs*, *idi*, and *ispDF*—were integrated into the genome of the chassis strain *Escherichia coli* MG1655 using a CRISPR-Cpf1-based system, resulting in MEP pathway-overexpressed strains. Additionally, the downstream module (MBot) of the mevalonate (MVA) pathway was optimized by introducing T7 RNA polymerase, *mvaE*, and *mvaS* from different species, including *Saccharomyces cerevisiae*, *Streptococcus pneumoniae*, and *Staphylococcus aureus*. Integration of the MEP genes improved lycopene production by 2 mg/L compared with the initial strain. Notably, fermentation performance varied significantly depending on the source of the downstream MBot module. The optimal combination—*erg12* from *Saccharomyces cerevisiae*, *mvaK* and *mvd1* from *Streptococcus pneumoniae*, and *idi* from *Escherichia coli*—achieved a lycopene titer of 86 mg/L in shake-flask cultures, representing a 21-fold increase compared to the parental strain. Paradoxically, *dxr* deletion to eliminate endogenous MEP flux precipitated a 7-fold drop in lycopene titre, whereas MEP overexpression failed to enhance production—revealing that MEP–MVA pathway synergy, rather than simple precursor supply, governs efficient carotenoid biosynthesis.

Citation: Xia W, Li W, Yao Q, Chen J. 2026. A metabolic optimization strategy based on modular genomic integration of the MVA pathway to enhance lycopene production in *Escherichia coli*. *Food Innovation and Advances* 5(2): 251–260 https://doi.org/10.48130/fia-0026-0017

Introduction

Terpenoids are a structurally diverse group of natural products with broad applications in pharmaceuticals, personal care, and agriculture[1]. Lycopene, a naturally occurring tetraterpenoid belonging to the carotenoid family, initially received limited attention due to its lack of provitamin A activity, unlike β-carotene. However, its strong antioxidant capacity and health benefits—such as antitumor effects and protection against prostate and cardiovascular diseases[2–5]—have expanded its use in cosmetics, nutraceuticals, and food products[6,7]. As demand for lycopene grows, developing cost-effective production methods has become a key research focus. Current approaches include plant extraction, chemical synthesis, and microbial fermentation. Plant extraction is limited by low yield, instability, and complex purification[8,9], while chemical synthesis faces issues with residual chemicals and lycopene degradation under heat and oxidative conditions[10]. In contrast, microbial fermentation has emerged as a promising alternative, enabled by advances in metabolic engineering and synthetic biology. This approach offers a more sustainable, environmentally friendly, and economically viable means of lycopene production[11]. To achieve this strategy, it is necessary to select efficient microbial hosts. *Escherichia coli* (*E. coli*) is one of the most widely used microbial hosts for heterologous terpenoid biosynthesis due to its well-characterized genetics, rapid growth, and ease of manipulation. Comparative lineage analyses reveal that K-12 strains outperform B strains for terpenoid production: their central carbon metabolism preferentially channels pyruvate and glyceraldehyde-3-phosphate into isoprenoid precursors, whereas B strains divert flux toward phosphoenolpyruvate synthesis and gluconeogenesis[12–14].

To increase the production of lycopene, increasing the intracellular supply of its precursors—isopentenyl pyrophosphate (IPP) and dimethylallyl pyrophosphate (DMAPP)—is a key strategy. These universal building blocks for terpenoid biosynthesis can be synthesized either via the endogenous methylerythritol phosphate (MEP) pathway or a heterologously introduced mevalonate (MVA) pathway (Fig. 1). Enhancing the supply of these precursors is crucial for improving terpenoid yields[15].

Within the MEP pathway, *dxs* encodes the rate-limiting enzyme and is frequently targeted to boost pathway flux[16,17]. Overexpression of *idi* helps balance the IPP/DMAPP ratio, further enhancing terpenoid biosynthesis[18]. Under normal growth conditions, both *dxs* and *idi* are expressed at low levels, and their co-overexpression further promotes terpenoid production[19,20]. Ajikumar et al. employed a modular metabolic engineering approach to overexpress *dxs*, *idi*, *ispD*, and *ispF*, which increased taxadiene production approaching 1 g/L in *E. coli*[21]. In addition to its role in isoprenoid biosynthesis, the MEP pathway also contributes to the oxidative stress response in *E. coli*[22].

The upstream MVA module (MUp), comprising *mvaE* and *mvaS*, synthesizes mevalonate, a key intermediate[23]. The downstream MVA module (MBot), including *mvaK1*, *mvaK2*, and *mvaD*, is also essential for efficient pathway operation. *mvaK1* is recognized as a regulatory bottleneck[24], and replacement with high-activity

© The Author(s)

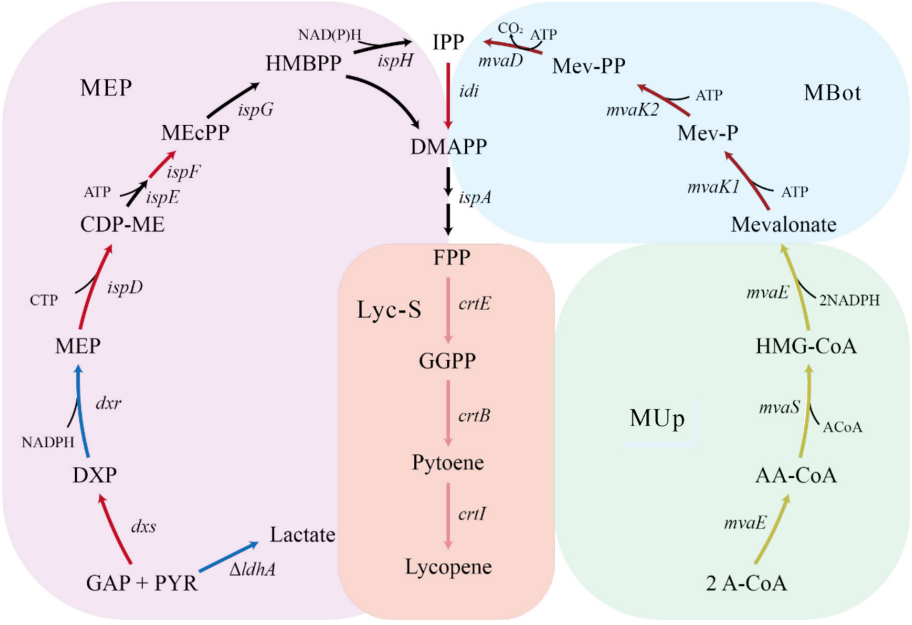

Fig. 1 Metabolic pathway for lycopene biosynthesis. GAP, glyceraldehyde-3-phosphate; PYR, pyruvate; DXP, 1-deoxy-D-xylulose-5-phosphate; MEP, methylerythritol-4-phosphate; CDP-ME, 4-diphosphocytidyl-2-C-methyl-D-erythritol; MEcPP, 2-C-methyl-D-erythritol-2,4-cyclodiphosphate; HMBPP, 2-Chydroxymethylbutenyl-4-diphosphate; IPP, isopentenyl pyrophosphate; DMAPP, dimethylallyl pyrophosphate; A-CoA, acetyl-CoA; AA-CoA, acetoacetyl-CoA; HMG-CoA, 3-hydroxy-3-methylglutaryl-CoA; Mevalonate, mevalonic acid; Mev-P, mevalonate-5-phosphate; Mev-PP, mevalonate-5-pyrophosphate; FPP, farnesyl pyrophosphate; GGPP, geranylgeranyl pyrophosphate; Phytoene, phytoene. Enzyme abbreviations: *dxs*, DXP synthase; *dxr*, DXP reductoisomerase; *ispD*, *ispE*, *ispF*, MEcPP synthase complex; *ispG*, MEcPP lyase; *ispH*, HMBPP reductase; *idi*, IPP isomerase; *ispA*, FPP synthase; *crtE*, GGPP synthase; *crtB*, phytoene synthase; *crtI*, phytoene desaturase; *mvaE*, cetoacetyl-CoA thiolase; *mvaS*, HMG-CoA synthase; *mvaK1*, mevalonate kinase; *mvaK2*, mevalonate-5-phosphate kinase; *mvaD*, mevalonate-5-pyrophosphate decarboxylase.

isozymes, such as *mvaK1* from *Staphylococcus aureus* (*S. aureus*), can substantially boost pathway flux in protoilludene production[25,26]. However, the MVA pathway typically involves the expression of multiple heterologous genes, traditionally delivered via plasmid-based systems. These systems are often plagued by genetic instability, antibiotic dependence, and increased metabolic burden on the host[19]. With the emergence of genome editing technologies, genomic integration of the MVA pathway has become a feasible alternative[27]. This approach improves genetic stability, reduces antibiotic usage, and shows better performance in long-term cultivation compared to plasmid-based systems[28,29].

In this study, modules of MVA from different sources were integrated into the genome of *E. coli* to evaluate their effects on lycopene production. The individual contributions of the MEP and MVA pathways to lycopene biosynthesis were also quantified. The genome-integration strategy developed in this study provides a practical and environmentally friendly approach for industrial-scale terpenoid production, addressing key limitations of plasmid-based expression systems. Moreover, these findings provide valuable insights and a technical reference for future efforts in microbial terpenoid biosynthesis.

Materials and methods

Bacterial strains and culture conditions

The bacterial strains used in this study are listed in Table 1. *E. coli* MG1655 was engineered for lycopene biosynthesis, while *E. coli* DH5α competent cells (Shanghai Wedi Biotechnology Co., Ltd., China) were used for recombinant plasmid construction. Strain activation and construction were carried out in LB medium (NaCl 10.00 g/L; yeast extract 5.00 g/L; tryptone 10.00 g/L) with solid medium supplemented with 1.8% (w/v) agar. Cultures were incubated at 37 °C for 12 h. Lycopene synthesis was conducted in fermentation medium (FJM) composed of tryptone (15.00 g/L), yeast extract (12.00 g/L), NaH_2PO_4 (2.23 g/L), Na_2HPO_4 (11.55 g/L), NaCl (2.50 g/L), Tween 80 (5.00 g/L), glycerol (20.00 g/L), $MgSO_4$ (0.50 g/L), and L-arabinose (1.50 g/L). $MgSO_4$, glucose, and L-arabinose were added as sterile stock solutions.

Plasmid constructions

Primers and sequencing services were provided by Beijing Qingke Biotechnology, China. Plasmid homologous recombination was performed using the Uniclone One Step Seamless Cloning Kit. Primers were designed to contain a 15–25 bp homologous sequence to ensure the efficiency of homologous recombination. The lycopene biosynthesis genes *crtB*, *crtI*, and *crtE* of *Pantoea ananatis* (*P. ananatis*) were synthesized by Jiangsu Genecefe Biotechnology Co., Ltd., China. Host strains used for heterologous gene sourcing included *Enterococcus faecalis* (*E. faecalis*, Ef), *S. aureus* (Sa), and *Bacillus subtilis* (*B. subtilis*, Bs), all maintained as laboratory stocks. *Streptococcus pneumoniae* (*S. pneumoniae*, Sp; GenBank: GCA_000007045.1) was kindly provided by Prof. Jie Feng of the Institute of Microbiology, Chinese Academy of Sciences. *Saccharomyces cerevisiae* (*S. cerevisiae*, Sc; GenBank: GCA_000146045.2) was provided by Dr. Dan Liu of China Agricultural University. All gene sequences used in this study are listed in Supplementary Table S1.

The *crtB-crtI-crtE* (*crtBIE*) module was assembled sequentially into pTrc99a and pGex-4T-2, with ribosome binding sites (RBS) inserted between stop and start codons to yield pTrc99a-crtBIE and pGex-crtBIE. The MEP pathway genes (*dxs*, *idi*, *ispDF*) were cloned into pTrc99a to construct pTrc99a-MEP. The upstream MVA module

Table 1. Strains constructed in this study.

Name	Description	Origin
DH5α	F$^-$ φ80 *lac* ZΔM15 Δ(*lacZYA-argF*) U169 *endA1 recA1 hsdR17*(rk$^-$, mk$^+$) *supE44* λ^- thi$^-$ *gyrA96 relA1 phoA*	Lab stock
MG1655	Wild-type	Lab stock
MG1655-pTrcBIE	MG1655 harbouring pTrc-crtBIE	This study
MG1655-pGexBIE	MG1655 harbouring pGex-crtBIE	This study
AME	MG1655 Δ*AraA*:: Ptrc-dxs-idi-ispDF containing pGex-crtBIE	This study
PME	MG1655 containing pcrEG-TrcMEP, pGex-crtBIE	This study
PAME	AME containing pcrEG-TrcMEP	This study
MGT7	MG1655 Δ*AraB*::T7 RNAP	This study
MGT7E	MGT7 Δ*lpxM*::T7 *lac MvaES*	This study
MGT7EE	MGT7 Δ*araA*::T7 *lac MvaES*	This study
MGT7E-pRSF-SaMBot	MGT7E harbouring pRSF-SaMBot	This study
MGT7E-pRSF-ScMBot	MGT7E harbouring pRSF-ScMBot	This study
MGT7E-pRSF-SpMBot	MGT7E harbouring pRSF-SpMBot	This study
MGT7E-pRSF-PTrcSpMBot	MGT7E harbouring pRSF-PtrcSpMBot	This study
MGT7E-pRSF-PGexSpMBot	MGT7E harbouring pRSF-PgexSpMBot	This study
MGT7E-pRSF-PVegSpMBot	MGT7E harbouring pRSF-PvegSpMBot	This study
MGT7E-pRSF-pJ23119SpMBot	MGT7E harbouring pRSF-PJ23119SpMBot	This study
MGT7EK$_{sa}$	MGT7E Δ*ldhA*::T7 *lac* SaMBot	This study
MGT7EK$_{sp}$	MGT7E Δ*ldhA*::T7 *lac* SpMBot	This study
MGT7EK$_{sc}$	MGT7E Δ*ldhA*::T7 *lac* ScMBot	This study
MGT7EK$_{saSp}$	MGT7E Δ*ldhA*::T7 *lac* SaSpMBot (*mvaK1* from *S.aureus* and *mvaK2*/*mvaD* from *S. pneumoniae*)	This study
MGT7EK$_{scSp}$	MGT7E Δ*ldhA*::T7 *lac* ScSpMBot (*erg12* from *S.cerevisiae* and *mvaK2*/*mvaD* from *S. pneumoniae*)	This study
MGT7EK$_{saSc}$	MGT7E Δ*ldhA*::T7 *lac* SaScMBot (*mvaK1* from *S.aureus* and *mvaK2*/*mvaD* from *S.cerevisiae*)	This study
MGT7EEK$_{sp}$	MGT7EE Δ*ldhA*::T7 *lac* SpMBot	This study
MGT7EEK$_{sc}$	MGT7EE Δ*ldhA*::T7 *lac* ScMBot	This study
MGT7EEK$_{sc}$Sp	MGT7EE Δ*ldhA*::T7 *lac* ScSpMBot (*erg12* from *S.cerevisiae* and *mvaK2*/*mvaD* from *S. pneumoniae*)	This study
MGT7EK$_{sc}$ dM	MGT7EK$_{sc}$ Δ*dxr*	This study
MGT7EKSp dM	MGT7EK$_{sp}$ Δ*dxr*	This study
MGT7EK$_{scSp}$dM	MGT7EK$_{scSp}$ Δ*dxr*	This study
AMET7EK$_{scSp}$	MGT7EK$_{scSp}$ ΔAraA::Ptrc-dxs-idi-ispDF	This study

(MUp) containing *mvaE* and *mvaS* was amplified from *E. faecalis* genomic DNA and cloned into pCDFDuet to produce pCDF-MUp. Three downstream MVA modules (MBot) were constructed in pRSF-Duet, each incorporating genes from different donor species. The SaMBot module consisted of *mvaK1*, *mvaK2*, and *mvaD* from *S. aureus*, along with *idi* from *E. coli*. The ScMBot module included *erg12*, *erg8*, and *erg19* from *S. cerevisiae*, together with *idi* from *E. coli*. The SpMBot module comprised *mvk*, *mvd1*, and *mvaK2* from *S. pneumoniae*, in combination with *idi* from *E. coli*. The schematic diagram for constructing the pcrEG vector employed in the CRISPR system is presented in Supplementary Fig. S1. All plasmids constructed in this study are summarized in Supplementary Table S2. The PAM sequences for CRISPR were predicted using the online tool CRISPR RGEN Tools. The PAM sequences corresponding to the target gene loci used in this study are listed in Supplementary Table S3.

Flask batch culture protocol and lycopene extraction

Strains were precultured overnight in LB at 37 °C, 220 r/min, then fermentation broth was prepared by transferring 1 mL of the preculture to a 100-mL FJM in 250 mL flasks. When OD_{600} reached approximately 0.25, 10 mM L-arabinose was added. When OD_{600} reached approximately 1.0, 0.2 mM IPTG was added, and cultivation continued at 30 °C, 220 r/min. As described by Yoon et al., lycopene was extracted and measured from *E. coli* using their established protocol[30]. Briefly, 1 mL of culture was centrifuged at 13,000 rpm for 3 min, and the cell pellet was washed with distilled water. The cells were then extracted with acetone at 55 °C in the dark for 15 min, followed by a second centrifugation. Lycopene content was quantified by measuring absorbance at 474 nm using a UV-2100 spectrophotometer (Unico, Shanghai, China). Each sample was subjected to three biological replicates simultaneously. Concentrations were calculated based on a standard curve (y = 0.2532x + 0.0073, R^2 = 0.9999; Supplementary Fig. S2).

Preparation of competent cells and genome editing

Competent cells were prepared using the calcium chloride method. Overnight cultures were inoculated (1% v/v) into 50 mL LB medium and grown at 37 °C with shaking at 220 rpm until the OD_{600} reached 0.2–0.3. L-arabinose was then added to a final concentration of 10 mM to induce expression, and cultivation continued until the OD_{600} reached approximately 0.6. Cells were chilled on ice for 30 min, harvested by centrifugation at 4 °C and 4,200 rpm for 6 min, and washed twice with ice-cold 0.1 M $CaCl_2$. The final pellet was resuspended in 0.1 M $CaCl_2$ containing 20% glycerol and stored at −80 °C. Genome editing was performed using the CRISPR/Cpf1 two-plasmid system, as described by Liu et al.[27]. Competent cells harboring the pEcCpf1 plasmid were electroporated with 500–1,000 ng of pcrEG and plated on selective media, followed by incubation at 37 °C for 24 h. Colonies were screened by colony PCR and confirmed by Sanger sequencing. Positive clones were cured of pcrEG plasmids by inducing with 0.1 mM rhamnose and subsequently cured of pEcCpf1 using 5 g/L glucose and 10 g/L sucrose.

Growth curve analysis

Single colonies were inoculated into 5 mL of FJM medium supplemented with appropriate antibiotics and cultured overnight at 37 °C

with shaking at 220 rpm. The overnight cultures were diluted to an initial OD_{600} of 0.5 and then inoculated (1:100) into 100 mL of fresh FJM in 250 mL Erlenmeyer flasks. Cell growth was monitored by measuring OD_{600} at 3-h intervals using a UV-2100 spectrophotometer (Unico, Shanghai, China).

Intracellular redox potential and ATP assay

The intracellular redox potential was measured using the Alamar Blue assay, with *E. coli* MG1655 as the negative control. Cultures grown to $OD_{600} \approx 0.6$ were diluted 10^3–10^4-fold and mixed at a 1:1 ratio with fully reduced Alamar Blue reagent in 96-well plates ($n = 6$). Plates were incubated in the dark at 37 °C for 4–6 h. Absorbance at 570 and 600 nm was recorded to calculate redox changes.

Intracellular ATP levels were determined using a commercial ATP assay kit (Beyotime Biotechnology, Shanghai, China), following the manufacturer's instructions. Cultures at $OD_{600} \approx 0.6$ were sampled in triplicate, and MG1655 was used as a reference strain.

Statistical analysis

Descriptive statistics and hypothesis testing were performed using GraphPad Prism 10. All experiments were independently repeated at least three times, and results are presented as mean ± standard deviation (SD). Differences among groups were analyzed using one-way repeated measures ANOVA. Post hoc multiple comparisons were conducted using Duncan's multiple range test with a significance level of $\alpha = 0.05$.

Results and discussion

Construction of the initial lycopene-producing strain and enhancement of the MEP pathway for improved production

To construct an initial strain capable of lycopene biosynthesis, the exogenous genes *crtB*, *crtI*, and *crtE* were cloned into the expression vectors pTrc99a and pGEX-4T-1, resulting in two lycopene biosynthesis expression constructs, pTrc99a-crtBIE and pGex-crtBIE. These constructs were transformed into *E. coli* MG1655 and subjected to shake flask fermentation. As shown in Fig. 2a, the strain harboring pGex-crtBIE produced 4 mg/L of lycopene, significantly higher than pTrc99a-crtBIE ($p < 0.0001$). Thus, pGex-crtBIE was selected as the lycopene biosynthetic module for subsequent experiments.

To increase lycopene yield, the endogenous methylerythritol-phosphate (MEP) pathway was augmented by either chromosomal integration or plasmid-based overexpression of *dxs*, *idi*, and *ispDF*, yielding the engineered strains AME (chromosomal integration), PME (plasmid expression), and PAME (combined chromosomal and plasmid overexpression). Fermentation results showed that lycopene production was elevated in all engineered strains (Fig. 2b), with AME showing the highest increase of approximately 2 mg/L. Relative to the chromosomally engineered CIBTS1557 strain (Yang et al.; 3.9 mg/L with co-overexpressed *ispGH*), our MEP-augmented chassis achieved 6.0 mg/L—a ~50% improvement that likely reflects optimized ribosome binding site strengths enhancing translational efficiency[31]. This improvement is likely attributable to the use of a stronger RBS set that elevates translational efficiency of the MEP-pathway enzymes. In contrast, plasmid-based overexpression of MEP genes showed minimal effect, indicating that genome-level enhancement is more effective than plasmid-based expression. However, the limited yield improvement suggests that further enhancement requires the introduction of an exogenous pathway.

Comparison of MVA downstream modules from different sources

Given that intracellular carbon flux restricts the MEP pathway's capacity for lycopene synthesis[32], and incorporating the MVA pathway into *E. coli* has been shown to significantly improve terpenoid production[14,30,33]. This study aimed to enhance precursor availability by introducing a heterologous MVA pathway. To assess the compatibility of MVA downstream modules (MBot) from different organisms, MBot from *S. cerevisiae* (ScMBot), *S. aureus* (SaMBot), and *S. pneumoniae* (SpMBot) were introduced into the host via the plasmid pRSFduet. It is worth noting that the *araB* gene in *E. coli* MG1655 was replaced with T7 RNA polymerase, enabling L-arabinose-inducible expression of MVA genes under the T7 promoter to prevent metabolic burden from toxic intermediates. The obtained strain was designated as MGT7 (Fig. 3a). The regulatory characteristics of this system (Supplementary Fig. S3) were validated using a GFP reporter plasmid (pet28a-sGFP). The results demonstrated minimal leaky expression in the absence of L-arabinose and repression of expression in the presence of ≥ 3 g/L glucose, confirming excellent regulation.

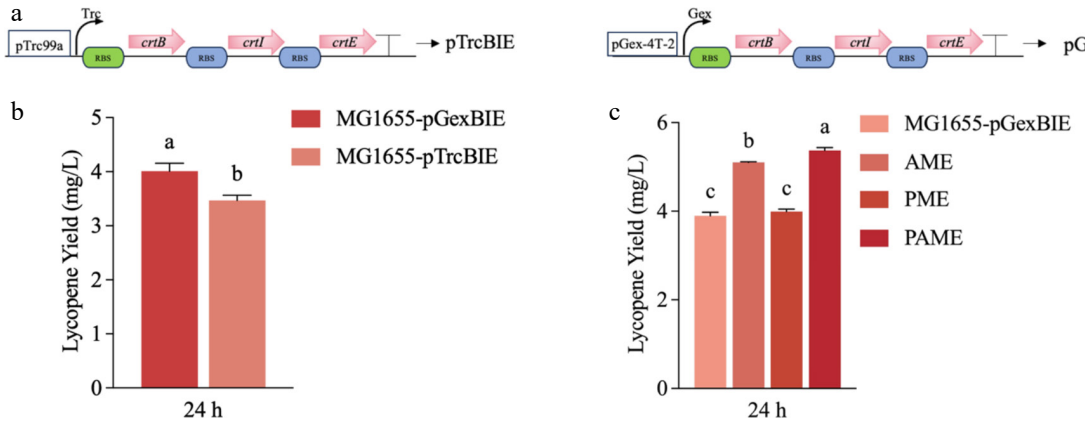

Fig. 2 Construction of the lycopene-synthesis module. (a) Genetic circuit diagrams of pTrcBIE and pGexBIE. *Trc* and *Gex* denote the *Trc* promoter and the *Gex* promoter, respectively, and a single arrow denotes one gene oriented 5′-3′. (b) Lycopene-producing capacities of pTrcBIE and pGexBIE in MG1655. (c) Effects of different MEP-pathway enhancement strategies on lycopene production. Values are means ± SD. Different lowercase letters (a, b, c) above the bars indicate significant differences among groups ($p < 0.05$).

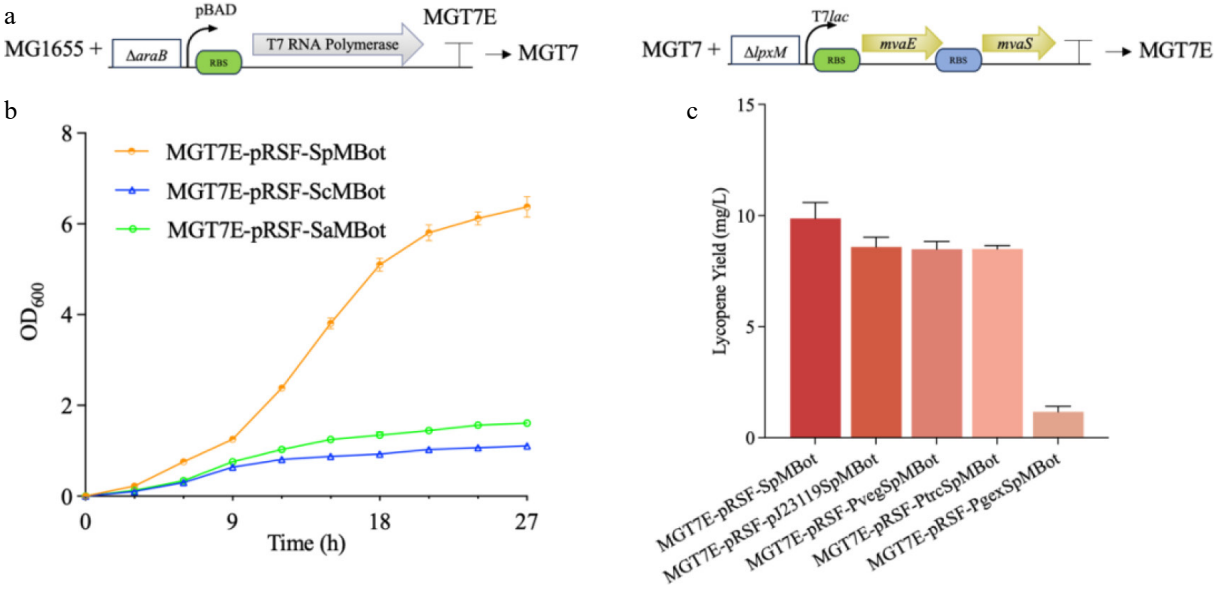

Fig. 3 Genomic integration of MUp and establishment of a plasmid-based MBot overexpression system. (a) Schematic depiction of the genomic integration sites and genetic circuits in the MGT7 and MGT7E strains. Green and blue rectangles indicate distinct RBS regions; Δ*araB* denotes replacement of the chromosomal *araB* gene with T7 RNA polymerase; Δ*lpxM* indicates substitution of the *lpxM* gene with the MUp module. *T7lac* represents the T7-lac promoter, and each arrow represents a single gene oriented 5′-3′. (b) Effects of plasmid-based overexpression of MBot modules from different sources within pRSFduet on lycopene production. (c) Influence of promoter optimization for SpMBot in pRSFduet on lycopene synthesis.

Subsequently, by replacing the chromosomal *lpxM* gene—a built-in on/off switch for *E. coli* endotoxic activity and a commonly targeted locus in previous studies—with the MUp module in MGT7, the new strain MGT7E was constructed (Fig. 3a). Building on these observations, plasmid-based expression of these modules was then evaluated. Only strains expressing SpMBot retained normal growth and lycopene production (Fig. 3b), while those expressing ScMBot and SaMBot exhibited growth inhibition and failed to produce lycopene. Therefore, further plasmid-level optimization focused on SpMBot. Among the tested promoters, the T7 promoter showed relatively higher activity (Fig. 3c), likely due to tight regulation and low background expression, and was incorporated into the following expression constructs.

Optimization of combinatorial MVA pathways

Plasmid-based expression of MVA downstream modules (MBot) from diverse origins conferred only a marginal increment in lycopene titer, a limitation that is further compounded by well-documented genetic instability inherent to plasmid-borne expression systems[19]. Therefore, these modules were integrated into the ldhA locus of the genome (Fig. 4a). On the one hand, *ldhA* encodes a key enzyme in the competing metabolic pathway, and thus its deletion could enhance the metabolic flux of the target pathway. On the other hand, previous studies have validated *ldhA* as an efficient integration site with favorable outcomes, and the results obtained in this study further confirmed that this locus exerted a significant positive effect on lycopene production (Fig. 4b)[29,31]. Among the resulting strains, MGT7EK$_{Sp}$ exhibited the highest lycopene production capacity, reaching 36 mg/L—significantly higher than that of strains harboring MBot from other sources (Fig. 4b). In contrast, MGT7EK$_{Sa}$ did not show a notable improvement in lycopene yield. From a fermentation time perspective, MGT7EK$_{Sc}$ produced more lycopene than MGT7EK$_{Sp}$ during the early fermentation phase (first 48 h) and reached its maximum yield within 48 h. This observation suggests that ScMBot may have higher catalytic activity than SpMBot, whereas SpMBot exhibits more sustained catalytic performance. Based on these findings, we further conducted combinatorial optimization of different pathways to explore their interactions and overall effects on lycopene production.

As shown in Fig. 4c, optimization of MBot from different sources was performed using two strategies. Through a cross-optimization strategy, we obtained strains MGT7EK$_{SaSp}$, MGT7EK$_{ScSp}$, and MGT7EK$_{SaSc}$, while a parallel optimization strategy yielded strain MGT7EK$_{Sc}$K$_{Sp}$. The hybrid MGT7EK$_{ScSp}$ strain, combining *S. cerevisiae erg12* with *S. pneumoniae* downstream enzymes, achieved 86 mg/L (35.8 mg/g DCW)—a 21-fold improvement over the parental strain and titre parity with multi-copy genomic integrants, yet without their propensity for recombination-mediated instability (Fig. 4d). This value is comparable to titers obtained with multi-copy genomic integration[29], while eliminating the elevated risk of intramolecular homologous recombination that progressively undermines genetic stability. Although the 86 mg/L titer was obtained in shake flasks, the resulting strain and operational parameters now provide a well-defined starting point for subsequent bioreactor characterization, which is scheduled as the next phase of this project.

This result strongly indicated that the *erg12* gene from *S. cerevisiae* plays a key role in the MVA pathway and that its synergistic optimization can significantly boost lycopene production. This is consistent with previous findings that *mvaK1*, a key enzyme in the MVA pathway, directly influences pathway flux[24], and the fermentation titer peaked at approximately 72 h[34]. Conversely, the low yield of MGT7EK$_{Sc}$K$_{Sp}$ suggested that simply combining two pathways did not necessarily promote lycopene synthesis. This may be due to excessive accumulation of intermediates or overexpression of multiple enzymes, imposing a substantial metabolic burden on the strain and thereby hindering efficient lycopene biosynthesis.

Comparative survey of *idi* sources for balancing isoprenoid precursors in *E. coli*

As key intermediates in the terpenoid biosynthetic pathway, the equilibrium between IPP and DMAPP plays a critical role in modulating the conversion efficiency to downstream products[18].

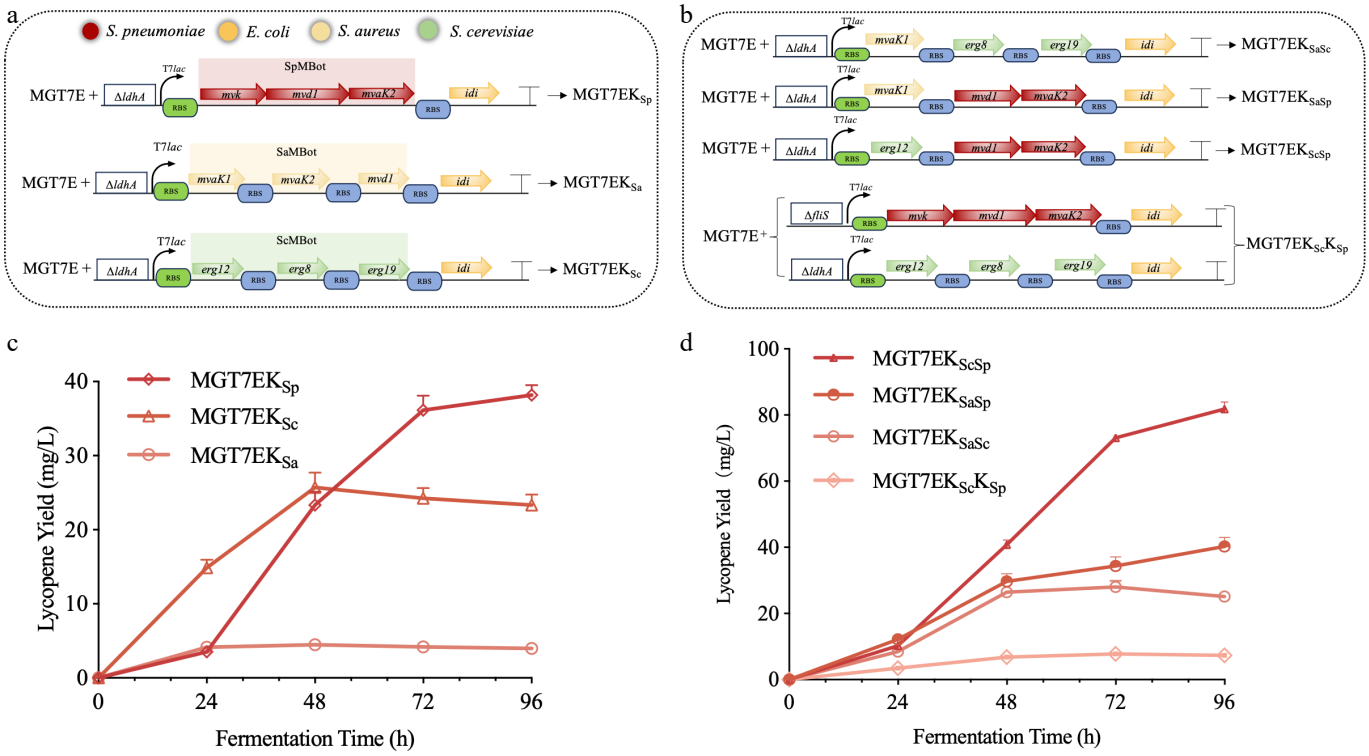

Fig. 4 Genomic integration and optimization of MBot modules from diverse origins. (a) Schematic representation of the genomic integration loci and genetic circuits for MBot modules from different sources. Δ*ldhA* indicates replacement of the *ldhA* gene with the corresponding MBot cassette. Green and blue rectangles denote distinct RBS regions; *T7lac* represents the T7-lac promoter; each arrow represents a single gene oriented 5′-3′. Colors are keyed as follows: red—*S. pneumoniae*, orange—*Escherichia coli*, beige—*S. aureus*, green—*S. cerevisiae*. (b) Lycopene production profiles following genomic integration of MBot modules from the indicated sources. (c) Schematic overview of the distinct MBot optimization strategies. Square brackets denote simultaneous integration of two pathways into the *fliS* and *ldhA* loci of the *MGT7E* genome. (d) Lycopene-producing capacities of strains constructed via the indicated MBot optimization strategies.

Disruption of this balance not only reduces product synthesis efficiency but may also inhibit strain growth. To investigate the influence of *idi*, which catalyzes the interconversion between IPP and DMAPP, the *idi* gene in MGT7EK$_{ScSp}$ was replaced with orthologs from *S. cerevisiae* (Scl), *S. aureus* (Sal), *S. pneumoniae* (Spl), *B. subtilis* (Bsl), and *E. faecalis* (Efl), yielding strains MGT7EK$_{ScSp}$Scl, MGT7EK$_{ScSp}$Sal, MGT7EK$_{ScSp}$Spl, MGT7EK$_{ScSp}$Bsl, and MGT7EK$_{ScSp}$Efl (Fig. 5a). Fermentation results (Fig. 5b) showed that the *E. coli idi* present in the parental strain was the most effective. Replacement with orthologs from other organisms led to reduced yields, underscoring the importance of balanced isoprenoid precursor supply for efficient lycopene biosynthesis.

MUp enhancement and balancing of MBot modules

It was shown that the enhancement of the Mup module can effectively promote the metabolic efficiency of the MVA pathway[29,31]. In this study, an additional Mup module was further introduced into three high-yield strains to enhance IPP/DMAPP precursor supply and improve substrate availability. As shown in Fig. 6a, b, compared with the MGT7EK$_{Sc}$ strain containing a single-copy Mup module, MGT7EEK$_{Sc}$ exhibited a significant increase in product concentration, reaching 43 mg/L, indicating a positive effect of module amplification. In contrast, the yield of MGT7EEK$_{Sp}$ was significantly reduced compared with its parental strain. This reduction was speculated to be associated with the relatively low catalytic activity of SpMBot during the first 48 h of cultivation, which may have prevented timely conversion of accumulated upstream intermediates, thereby causing metabolic stress accumulation, impairing cell growth, and ultimately suppressing product synthesis.

In comparison, ScMBot displayed stronger catalytic activity during the same time frame, enabling MGT7EEK$_{Sc}$ to efficiently convert upstream precursors, thereby alleviating metabolic burden and enhancing product yield. Moreover, MGT7EEK$_{ScSp}$ showed no significant change in yield under enhanced upstream flux, further confirming that ScMBot possesses superior metabolic capacity to SpMBot during the initial production phase. This observation aligns with previous findings that ScMBot has higher early-stage catalytic efficiency than SpMBot. It was further speculated that this advantage may be attributed not only to the *erg12* gene within ScMBot, but also to the enzymatic activities of *erg8* and *erg19*.

To further investigate why MGT7EEK$_{ScSp}$ did not exhibit a marked yield improvement, *erg12* and *idi* were assessed for remaining optimization potential, and *erg8* and *erg19* were examined as possible rate-limiting factors. For this purpose, the *erg12–idi* module (KI) or the *erg8–erg19* module (KD) was individually enhanced in the genomes of both MGT7EK$_{ScSp}$ and MGT7EEK$_{ScSp}$, yielding four recombinant strains: MGT7EK$_{ScSpKI}$, MGT7EK$_{ScSp}$KD, MGT7EEK$_{ScSp}$KI, and MGT7EEK$_{ScSp}$KD (Fig. 6c). Fermentation results revealed that neither KI nor KD modification produced a significant yield improvement in MGT7EEK$_{ScSp}$ (Fig. 6d), indicating that these modules were not key factors limiting its productivity.

Deletion and functional validation of *dxr*

The MEP pathway is essential in *E. coli*; its complete deletion has rarely been achieved in prior work. Although attempts have emerged

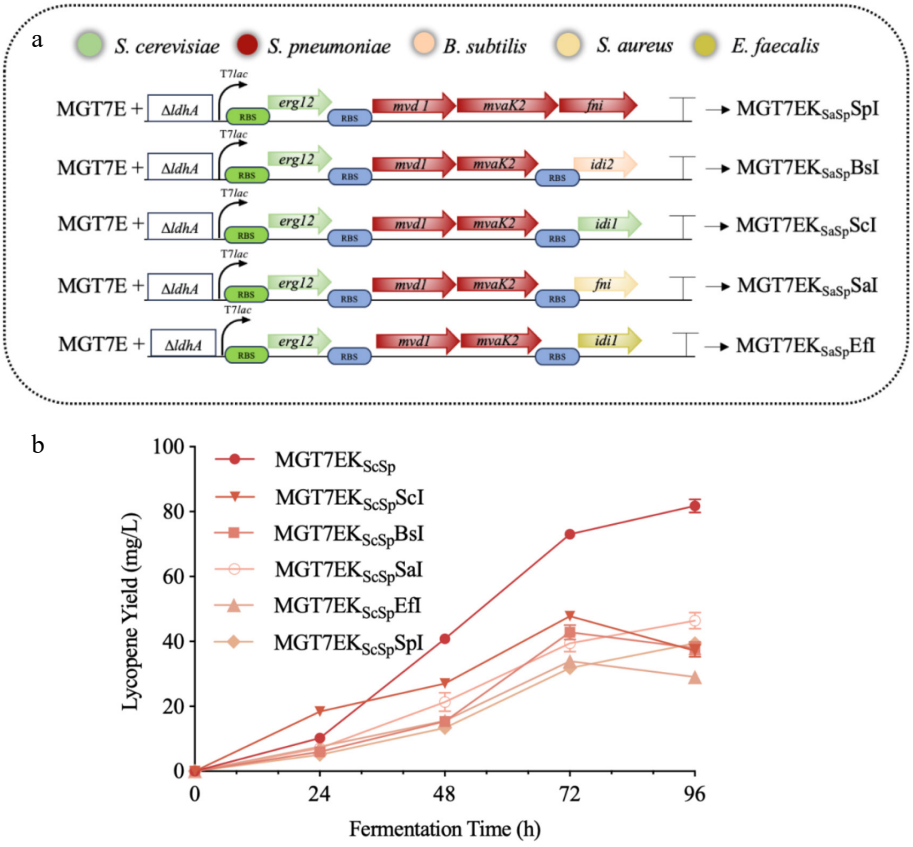

Fig. 5 Screening of *idi* orthologs from diverse sources. (a) Schematic diagram of the optimization strategies employing *idi* genes from multiple origins. Δ*ldhA* denotes replacement of the *ldhA* gene with the corresponding *MBot* cassette. Green and blue rectangles indicate distinct *RBS* regions; *T7lac* represents the *T7-lac* promoter; each arrow represents a single gene oriented 5′-3′. Colors correspond to the following sources: green—*S. cerevisiae*, red—*S. pneumoniae*, peach—*B. subtilis*, beige—*S. aureus*, chartreuse—*Enterococcus faecalis*. (b) Lycopene production profiles for strains harboring *idi* variants from the indicated sources.

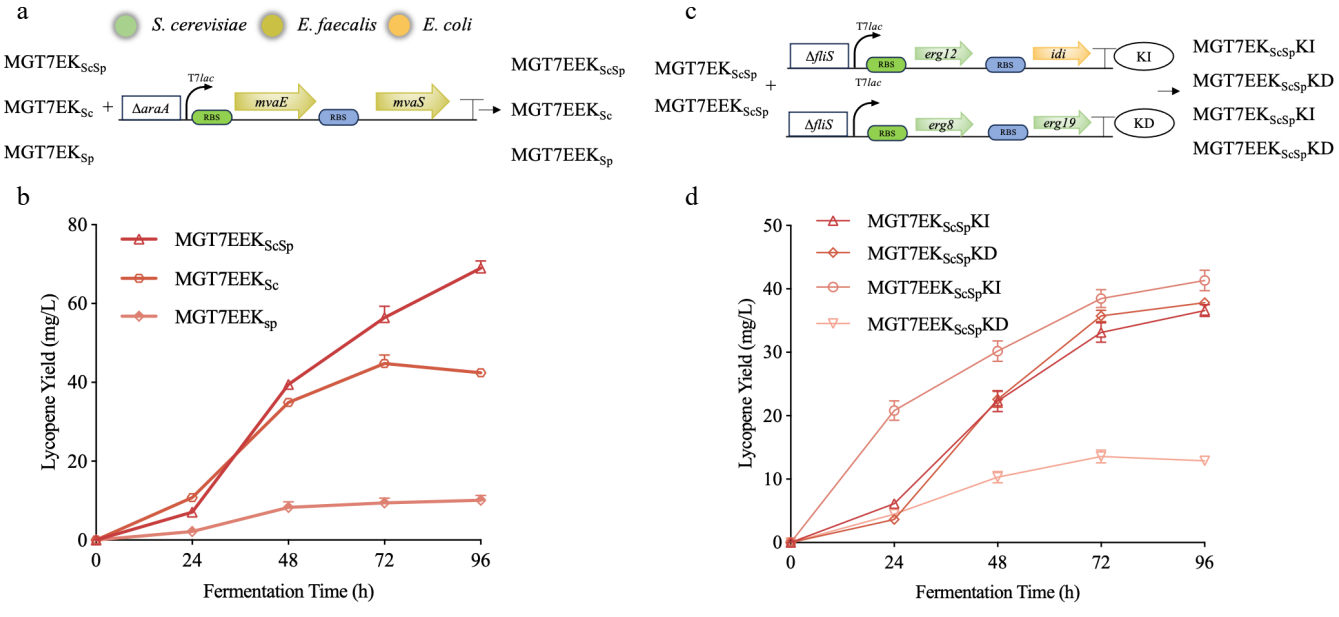

Fig. 6 Enhancement of MUp and synergistic optimization of MBot. (a) Schematic of MUp enhancement in the MGT7EK$_{ScSp}$, MGT7EK$_{Sc}$, and MGT7EK$_{Sp}$. Δ*araA* indicates replacement of the *araA* gene with the MUp module. Green and blue rectangles denote distinct RBS regions; *T7lac* represents the *T7-lac* promoter; each arrow represents a single gene oriented 5′-3′. Colors correspond to the following sources: green—*S. cerevisiae*, chartreuse—*Enterococcus faecalis*, orange—*Escherichia coli*. (b) Impact of MUp enhancement on lycopene production by different MBot modules. (c) Optimization strategies for MBot. KD and KI designate the corresponding modules in strain nomenclature; Δ*fliS* denotes replacement of the *fliS* gene with the indicated module. (d) Lycopene production profiles following MUp and MBot optimization.

in the past two years[35], whether the MEP and MVA pathways conflict with or complement each other remains unresolved. Therefore, in this study, the interaction between MEP and MVA pathways in *E. coli* was systematically investigated by overexpressing MEP genes and deleting the rate-limiting *dxr* gene in various MBot-integrated strains: MGT7EK$_{Sc}$, MGT7EK$_{Sp}$, MGT7EK$_{Sa}$, and MGT7EK$_{ScSp}$.

The *dxr* deletion was unsuccessful in MGT7EK$_{Sa}$, likely because SaMBot did not provide sufficient metabolic flux to compensate for the loss of *dxr*, resulting in lethal growth defects. Similarly, no positive clones were obtained for MGT7EK$_{Sc}$ overexpressing MEP, likely due to toxic intermediate accumulation caused by ScMBot's strong catalytic activity combined with elevated MEP flux.

Functional validation revealed that the *dxr* deletion significantly impaired growth in all three viable strains. Without L-arabinose induction, cultures exhibited severe growth arrest, especially MGT7EK$_{Sc}$, which remained transparent even after 30 h, suggesting that *dxr* is essential for *E. coli* viability. Although growth partially recovered with arabinose induction, it remained below that of non-deletion controls (Fig. 7a). Fermentation analysis (Fig. 7b) showed marked decreases in lycopene yield post-*dxr* deletion, with MGT7EK$_{ScSp}$dm dropping from 86 to 10 mg/L. As *dxr* is an indispensable component of the MEP pathway that dominates terpenoid biosynthesis in *E. coli*, this study then performed a complementary experiment by overexpressing the entire MEP pathway to explore whether enhancing the flux of this pathway could rescue or promote lycopene accumulation. Unexpectedly, in contrast to the inhibitory effect of *dxr* deletion, MEP overexpression had no significant effect on lycopene synthesis (Fig. 7c).

To elucidate the underlying metabolic differences, intracellular redox status and ATP levels were assessed. Except for MGT7EK$_{Sp}$, *dxr* deletion significantly reduced NAD(P)H levels (Fig. 7e). ATP levels followed a similar trend (Fig. 7d), highlighting the importance of the MEP pathway in cellular redox and energy homeostasis. Thus, while MEP augmentation failed to boost lycopene titres, it proved essential for maintaining cellular bioenergetic capacity—indicating that *dxr* and other MEP nodes warrant preservation even when a heterologous MVA pathway is operational. These findings align with recent proposals that the MEP pathway serves as a sentinel for stress perception, signal transduction, and cellular protection across diverse organisms[22]. Collectively, these data indicate that, while the MEP pathway may not directly boost product formation in *E. coli*, it is vital for maintaining robust cellular growth. Supplementation of the medium with L-arabinose partially restored the growth of our engineered Δ*dxr* strain, laying the groundwork for future mechanistic dissection of the MEP pathway.

Conclusions

In this study, key MVA-pathway enzymes from diverse organisms were screened and optimized, assembled into a single operon, and integrated as a one-copy insertion into the chromosome, resulting in an antibiotic-free, repeat-free *E. coli* chassis that stably and efficiently produces lycopene. Shake-flask fermentations revealed that the lycopene titer of this single-copy integrant matches the values previously reported for strains harboring multiple genomic copies, while the engineered strain grew as robustly as the parental control, thus circumventing the conventional liabilities of plasmid dependence and genomic instability.

To clarify the interplay between the MVA and MEP pathways, this study engineered an MVA-complete background carrying either the *dxr* deletion or MEP overexpression. MEP overexpression did not enhance lycopene titers, whereas *dxr* loss severely impaired growth and dramatically decreased yield, underscoring that the MEP pathway is irreplaceable for basal metabolic balance and energy

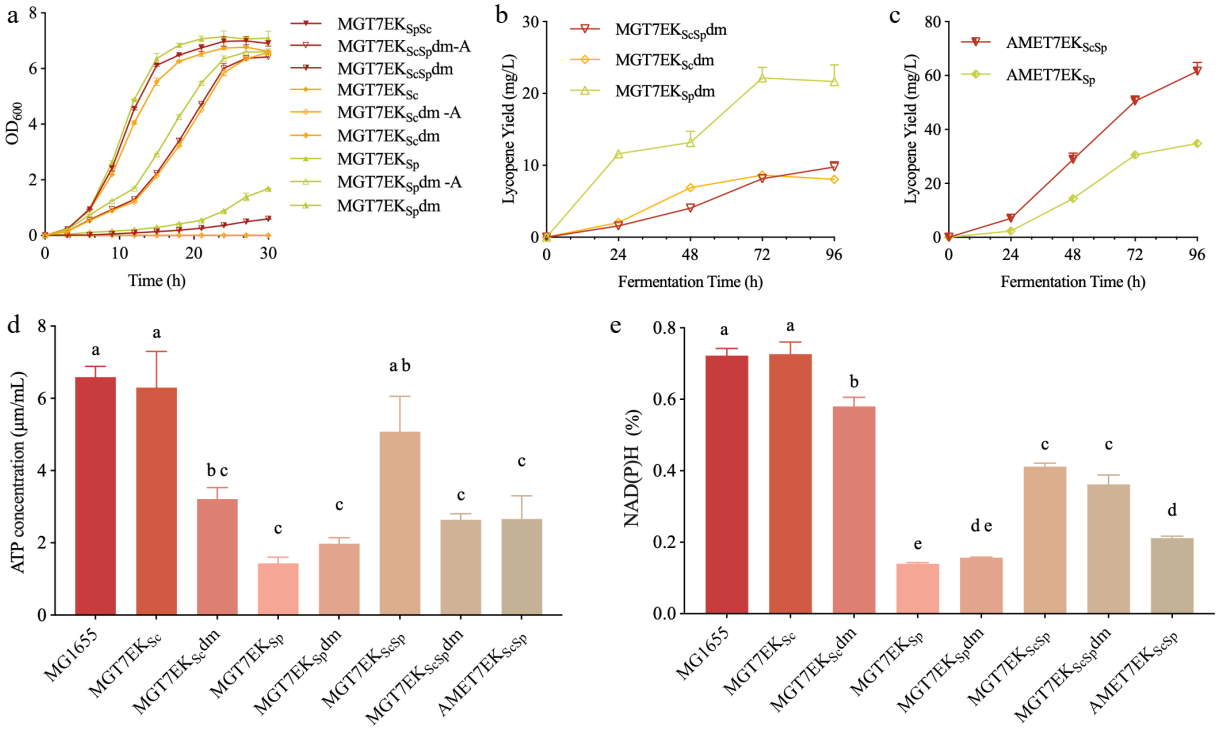

Fig. 7 Role of the MEP pathway in MVA-mediated lycopene synthesis. (a) Growth curves of MGT7EKScSp, MGT7EK$_{Sc}$, and MGT7EK$_{Sp}$ after deletion of the *dxr* gene; '–A' indicates medium supplemented with 0.2% L-arabinose, and 'dm' denotes *dxr* deletion. (b) Impact of *dxr* deletion on lycopene production. (c) Effect of MEP-pathway overexpression on lycopene synthesis. (d) Intracellular ATP levels in *dxr*-deleted and MEP-overexpressing strains. (e) Intracellular reducing-power levels in *dxr*-deleted and MEP-overexpressing strains.

homeostasis. This aligns with emerging evidence that the MEP pathway functions as a biosensor for oxidative stress, coupling metabolic state to stress signalling and cellular defence across kingdoms—a role that may supersede its canonical function in isoprenoid precursor supply[35]. In summary, this study provides a more stable strategy for lycopene synthesis in *E. coli* and successfully constructs an *E. coli* strain that is deficient in the *dxr* gene yet capable of normal growth, offering a defined genetic context for the mechanistic dissection of the MEP pathway.

Author contributions

The authors confirm their contributions to the paper as follows: study conception and design: Xia W, Chen J; data collection: Xia W; analysis and interpretation of results: Xia W, Li W, Yao Q; draft manuscript preparation: Xia W, Li W; writing – review and editing: Li W, Yao Q, Chen J; supervision: Yao Q, Chen J; funding acquisition, methodology, supervision: Chen J. All authors reviewed the results and approved the final version of the manuscript.

Data availability

All data generated or analyzed during this study are included in this published article and its supplementary information files.

Acknowledgment

This work was supported by the Key R&D Program of Shandong Province, China (Grant No. 2024TZXD013), Provincial and Municipal Agricultural Subsidy Special Funds for the Construction of CAU-SCCD Advanced Agricultural & Industrial Institute, and Project of National Center of Technology Innovation for Comprehensive Utilization of Saline-Alkali Land (Grant No. GYJ2023006). We sincerely thank Prof. Jie Feng (Institute of Microbiology, CAS) and Dr. Dan Liu (China Agricultural University) for kindly providing microbial genomic DNAs and giving valuable advice on the experimental methods.

Conflict of interest

The authors declare that they have no conflict of interest.

Supplementary information accompanies this paper online at: https://doi.org/10.48130/fia-0026-0017.

Dates

Received 15 December 2025; Revised 28 January 2026; Accepted 31 January 2026; Published online 19 May 2026

References

[1] Tetali SD. 2019. Terpenes and isoprenoids: a wealth of compounds for global use. *Planta* 249:1–8

[2] Maaz M, Sultan MT, Khalid MU, Raza H, Imran M, et al. 2025. A comprehensive review on the molecular mechanism of lycopene in cancer therapy. *Food Science & Nutrition* 13:e70608

[3] López-Solís R, Castro-Barquero S, Donat-Vargas C, Corrado M, Arancibia-Riveros C, et al. 2025. Lycopene intake and prostate cancer risk in men at high cardiovascular risk: a prospective cohort study. *BMC Medicine* 23:627

[4] Moran NE, Thomas-Ahner JM, Wan L, Zuniga KE, Erdman JW, et al. 2022. Tomatoes, lycopene, and prostate cancer: what have we learned from experimental models? *The Journal of Nutrition* 152:1381–1403

[5] Sharifi-Zahabi E, Soltani S, Malekahmadi M, Rezavand L, Clark CCT, et al. 2022. The effect of lycopene supplement from different sources on prostate specific antigen (PSA): a systematic review and meta-analysis of randomized controlled trials. *Complementary Therapies in Medicine* 64:102801

[6] Kulawik A, Cielecka-Piontek J, Zalewski P. 2023. The importance of antioxidant activity for the health-promoting effect of lycopene. *Nutrients* 15:3821

[7] Khan UM, Sevindik M, Zarrabi A, Nami M, Ozdemir B, et al. 2021. Lycopene: food sources, biological activities, and human health benefits. *Oxidative Medicine and Cellular Longevity* 2021:2713511

[8] Li L, Liu Z, Jiang H, Mao X. 2020. Biotechnological production of lycopene by microorganisms. *Applied Microbiology and Biotechnology* 104:10307–10324

[9] Nie X, Zuo Z, Zhou L, Gao Z, Cheng L, et al. 2024. Investigating the effect of high-voltage electrostatic field (HVEF) treatment on the physicochemical characteristics, bioactive substances content, and shelf life of tomatoes. *Foods* 13:2823

[10] Moroz P, Bartusiak A, Niewiadomska J, Szymański K, Janek T, et al. 2025. Advances in lycopene production: from natural sources to microbial synthesis using *Yarrowia lipolytica*. *Molecules* 30:4321

[11] Li M, Xia Q, Zhang H, Zhang R, Yang J. 2020. Metabolic engineering of different microbial hosts for lycopene production. *Journal of Agricultural and Food Chemistry* 68:14104–14122

[12] Ren J, Shen J, Thai TD, Kim MG, Lee SH, et al. 2023. Evaluation of various *Escherichia coli* strains for enhanced lycopene production. *Journal of Microbiology and Biotechnology* 33:973–979

[13] Boghigian BA, Salas D, Ajikumar PK, Stephanopoulos G, Pfeifer BA. 2012. Analysis of heterologous taxadiene production in K- and B-derived *Escherichia coli*. *Applied Microbiology and Biotechnology* 93:1651–1661

[14] Yoon SH, Lee SH, Das A, Ryu HK, Jang HJ, et al. 2009. Combinatorial expression of bacterial whole mevalonate pathway for the production of β-carotene in *E. coli*. *Journal of Biotechnology* 140:218–226

[15] Liang Z, Zhi H, Fang Z, Zhang P. 2021. Genetic engineering of yeast, filamentous fungi and bacteria for terpene production and applications in food industry. *Food Research International* 147:110487

[16] Banerjee A, Wu Y, Banerjee R, Li Y, Yan H, et al. 2013. Feedback inhibition of deoxy-D-xylulose-5-phosphate synthase regulates the methylerythritol 4-phosphate pathway. *Journal of Biological Chemistry* 288:16926–16936

[17] Hu B, Zhou J, Li J, Chen J, Du G, et al. 2025. Efficient biosynthesis of furanocoumarin intermediate marmesin by engineered *Escherichia coli*. *ACS Synthetic Biology* 14:954–966

[18] Li Y, Wang G. 2016. Strategies of isoprenoids production in engineered bacteria. *Journal of Applied Microbiology* 121:932–940

[19] Raghavan I, Juman R, Wang ZQ. 2024. The non-mevalonate pathway requires a delicate balance of intermediates to maximize terpene production. *Applied Microbiology and Biotechnology* 108:245

[20] Rehman E, Hawaibam BS, Nguyen MP, Wang C, Yoon SH, et al. 2025. Enhancing lycopene production in *Bacillus subtilis* by overcoming a critical enzymatic bottleneck. *Frontiers in Bioengineering and Biotechnology* 13:1670015

[21] Ajikumar PK, Xiao WH, Tyo KEJ, Wang Y, Simeon F, et al. 2010. Isoprenoid pathway optimization for taxol precursor overproduction in *Escherichia coli*. *Science* 330:70–74

[22] Perez-Gil J, Behrendorff J, Douw A, Vickers CE. 2024. The methylerythritol phosphate pathway as an oxidative stress sense and response system. *Nature Communications* 15:5303

[23] Liu CL, Dong HG, Xue K, Sun L, Yang Y, et al. 2022. Metabolic engineering mevalonate pathway mediated by RNA scaffolds for mevalonate and isoprene production in *Escherichia coli*. *ACS Synthetic Biology* 11:3305–3317

[24] Wang Y, Yu J, Zhang H, Xu M, Liu Q, et al. 2025. Shaping up a mevalonate pathway in the *E. coli–E. coli* coculture system for the production of sesquiterpenes. *Journal of Agricultural and Food Chemistry* 73:4820–4828

[25] Li M, Chen H, Liu C, Guo J, Xu X, et al. 2019. Improvement of isoprene production in *Escherichia coli* by rational optimization of RBSs and key enzymes screening. *Microbial Cell Factories* 18:4

[26] Yang L, Wang C, Zhou J, Kim SW. 2016. Combinatorial engineering of hybrid mevalonate pathways in *Escherichia coli* for protoilludene production. *Microbial Cell Factories* 15:14

[27] Zhu X, Wu Y, Lv X, Liu Y, Du G, et al. 2022. Combining CRISPR–Cpf1 and recombineering facilitates fast and efficient genome editing in *Escherichia coli*. *ACS Synthetic Biology* 11:1897–1907

[28] Hussain MH, Hong Q, Zaman WQ, Mohsin A, Wei Y, et al. 2021. Rationally optimized generation of integrated *Escherichia coli* with stable and high yield lycopene biosynthesis from heterologous mevalonate (MVA) and lycopene expression pathways. *Synthetic and Systems Biotechnology* 6:85–94

[29] Wei Y, Mohsin A, Hong Q, Guo M, Fang H. 2018. Enhanced production of biosynthesized lycopene *via* heterogenous MVA pathway based on chromosomal multiple position integration strategy plus plasmid systems in *Escherichia coli*. *Bioresource Technology* 250:382–389

[30] Yoon SH, Lee YM, Kim JE, Lee SH, Lee JH, et al. 2006. Enhanced lycopene production in *Escherichia coli* engineered to synthesize isopentenyl diphosphate and dimethylallyl diphosphate from mevalonate. *Biotechnology and Bioengineering* 94:1025–1032

[31] Yang C, Gao X, Jiang Y, Sun B, Gao F, et al. 2016. Synergy between methylerythritol phosphate pathway and mevalonate pathway for isoprene production in *Escherichia coli*. *Metabolic Engineering* 37:79–91

[32] Rinaldi MA, Ferraz CA, Scrutton NS. 2022. Alternative metabolic pathways and strategies to high-titre terpenoid production in *Escherichia coli*. *Natural Product Reports* 39:90–118

[33] Niu FX, Lu Q, Bu YF, Liu JZ. 2017. Metabolic engineering for the microbial production of isoprenoids: carotenoids and isoprenoid-based biofuels. *Synthetic and Systems Biotechnology* 2:167–175

[34] Liu N, Liu B, Wang G, Soong YV, Tao Y, et al. 2020. Lycopene production from glucose, fatty acid and waste cooking oil by metabolically engineered *Escherichia coli*. *Biochemical Engineering Journal* 155:107488

[35] Tan JC, Hu Q, Scrutton NS. 2024. A growth-coupling strategy for improving the stability of terpenoid bioproduction in *Escherichia coli*. *Microbial Cell Factories* 23:279

Copyright: © 2026 by the author(s). Published by Maximum Academic Press on behalf of China Agricultural University, Zhejiang University and Shenyang Agricultural University. This article is an open access article distributed under Creative Commons Attribution License (CC BY 4.0), visit https://creativecommons.org/licenses/by/4.0/.